Journal of Power Sources 203 (2012) 109–114

Contents lists available at SciVerse ScienceDirect

Journal of Power Sources

journal homepage: www.elsevier.com/locate/jpowsour

Raman study of structural stability of $LiCoPO_4$ cathodes in $LiPF_6$ containing electrolytes

R. Sharabi[a], E. Markevich[a,*], V. Borgel[a], G. Salitra[a], G. Gershinsky[a], D. Aurbach[a], G. Semrau[b], M.A. Schmidt[b], N. Schall[c], C. Stinner[c]

[a] Department of Chemistry, Bar-Ilan University, Ramat Gan 52900, Israel
[b] Merck KGaA, Frankfurter Straße 250, D-64293 Darmstadt, Germany
[c] Süd-Chemie AG, Ostenriederstraße 15, 85368 Moosburg, Germany

ARTICLE INFO

Article history:
Received 19 September 2011
Received in revised form 7 December 2011
Accepted 9 December 2011
Available online 17 December 2011

Keywords:
Lithium–cobalt phosphate
Olivines
Raman spectroscopy
Lithium batteries, Structural degradation

ABSTRACT

Micro-probe Raman spectroscopy investigation of $LiCoPO_4$ composite electrodes performed after prolonged cycling in $LiPF_6$ EC/DMC electrolyte solution revealed total structural degradation of the olivine structure of the electrodes. The electrodes cycled in the identical conditions but in the presence of the HF-scavenging glassy fiber (GF) separators retain their olivine structure unchanged. The reasons for this pronounced difference are discussed.

© 2011 Elsevier B.V. All rights reserved.

1. Introduction

Olivines $LiMPO_4$ (M = Fe, Mn, Co, or Ni) have been widely investigated as cathode materials for lithium batteries due to their high theoretical capacity and flat voltage profile [1]. $LiCoPO_4$ is the most attractive among these compounds from a view of high theoretical power density due to its high operating voltage of 4.8 V vs. Li/Li^+ and high theoretical capacity of 167 mAh g^{-1} [2]. High power density is a crucial factor for electric vehicle applications. Therefore, $LiCoPO_4$ is considered as one of the most promising high-voltage cathode materials for advanced Li ion batteries.

However, only 60–80% of its theoretical capacity can be obtained for this material in the initial discharge, and fast capacity fading of $LiCoPO_4$ electrodes is generally observed [3–8]. Several factors were argued to be responsible for the poor electrochemical performance of $LiCoPO_4$, including extremely low electronic conductivity and Li-ion diffusivity [9,10], electrolyte solution degradation due to the high working potential [11] and irreversible structural deformations [4]. To ensure better electronic conductivity, $LiCoPO_4$ for the electrodes preparation is most commonly used in a form of carbon-coated particles.

In the present work, we use Raman spectroscopy to follow structural changes of $LiCoPO_4$ electrodes as the result of their galvanostatic cycling. The presence of the carbon coating layer on the surface of $LiCoPO_4$ electrode materials attenuates the signal from the olivine structure and hampers the analysis of the spectral features of the bulk material. Recently, we showed [12] that at a moderate power of the laser beam the carbon coating layer can be removed from the surface of the $LiCoPO_4$ particles in air without damaging the structure of the underlying olivine. Here we use this approach for the study the structural stability and instability of $LiCoPO_4$ electrodes after their cycling in different conditions.

2. Experimental

Carbon-coated nano-powders of $LiCoPO_4$ (Table 1) were prepared by hydrothermal synthesis as described in [13]. The carbon content in the samples was determined by an Eager, Inc. Model 200 C, H, N, S analyzer. The surface area of the samples was calculated using the BET equation from the adsorption isotherm data, determined by N_2 gas adsorption at 77 K using an Autosorb-1-MP apparatus (Quantachrome Corporation). High resolution environmental scanning electron microscopy imaging, using a E-SEM Ouanta FEG instrument was performed to estimate the average particle size and morphology (Fig. 1).

The cathode sheets were fabricated by spreading slurry (a suspension of active cathode material powder and carbon black in a PVdF/N-methylpyrrolidon) on an aluminum foil current collector with a doctor blade device. Typically, the electrodes contained 3–4 mg of active mass. The electrolyte solution was 1 M of $LiPF_6$

* Corresponding author. Tel.: +972 3 531 7680; fax: +972 3 738 4053.
E-mail address: markeve@mail.biu.ac.il (E. Markevich).

0378-7753/$ – see front matter © 2011 Elsevier B.V. All rights reserved.
doi:10.1016/j.jpowsour.2011.12.018

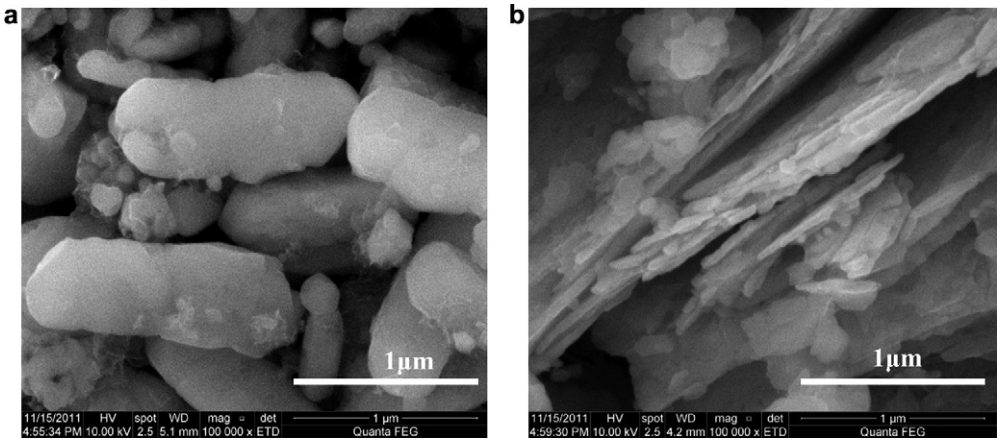

Fig. 1. SEM images of carbon coated $LiCoPO_4$ powders: (a) micro-powder and (b) nano-powder.

Table 1
Characteristics of the carbon-coated $LiCoPO_4$ powders.

	Carbon content (weight %)	BET surface area ($m^2\ g^{-1}$)
Micro-powder	1.2	1.4
Nano-powder	1.8	21

in an EC + DMC 1:1 mixture (Li-battery grade from Merck, KGaA). Two types of separators were used for the preparation of the cells, namely, a PE separator (Setela Tonen, Japan) and a glassy fiber (GF) separator (Glass-mat, Hollingsworth & Vose Co. Ltd., UK, BG03015 grade).

Two-electrode cells comprising $LiCoPO_4$ electrodes, separators, an electrolyte solution, and Li foil negative electrodes were assembled in a glove box filled with pure argon and sealed in 2032 coin-cells (NRC, Canada). Galvanostatic cycling of $LiCoPO_4$/Li cells was carried out using an Arbin model BT2000 multi-channel battery tester (Arbin Instruments, USA). At the end of cycling the cells were fully discharged to 3.5 V at C/5 and then potentiostatically at 3.5 V for 10 h. The discharged cells were disassembled in the glovebox, cathodes and separators were rinsed thoroughly with DMC and dried in the glovebox prior to Raman analysis.

Raman spectra were measured in a back scattering configuration using a micro-Raman spectrometer HR 800 (Jobin Yvon Horiba), with a He–Ne laser (excitation line 632.8 nm) and a microscope objective (50×, Olympus LWD). The power of the laser beam on the sample was varied between 0.37 and 4.3 mW. The diameter of the laser beam on the sample was ~1.4 µm.

3. Results and discussion

Typical cycling results of $LiCoPO_4$/Li cells for the electrodes prepared from micro- and nano-particles with two types of separators are shown in Fig. 2. It is seen that with both electrodes prepared from micro-powder and nano-powder of $LiCoPO_4$ the capacity retention is much better for the cells with GF separators than for the cells with ordinary PE separators. For the electrodes prepared from micro-material this effect is much more pronounced. After cycling, the cells were disassembled. Black precipitate from both cathode and anode side of the PE separators was observed. We performed micro-Raman analysis of these deposits to identify their composition. Typical micro-Raman spectra of the particles trapped in the PE separator are shown in Fig. 3. The main component both on the cathode and the anode side of the separators is disordered carbon with its D and G bands at about 1340 and 1580 cm^{-1}, respectively [14]. Besides that, other moieties that can be assigned as surface species formed on the electrodes were observed on both sides of the separators: On the cathode side the peak at 1097 cm^{-1} corresponds to Li_2CO_3 and the peak at 1477 cm^{-1} relates to lithium oxalate [15]. On the lithium side $CoCO_3$ was detected with its two Raman bands at 1089 cm^{-1} and 1437 cm^{-1} [16]. Thus, two main reasons for the phenomenon of the significantly faster capacity fading in the case of PE separator compared to the apparent better stability observed with use of GF separator can be considered. The first one is the mechanical clogging of the PE separator during cycling with carbon from the carbon coating layer of the $LiCoPO_4$ particles and the side products formed by the electrolyte solution decomposition. The second reason for such a difference between the impacts of the separators used can be a possible chemical activity of the GF separators towards some detrimental components which are present or are formed in the electrolyte solution during operation. To discriminate between these two possibilities the following experiment was performed: Initially, the cells were cycled with PE separators down to a significant capacity fading (Fig. 4a). After that, the cells were disassembled and the old separators were replaced by the fresh PE (Fig. 4a, black curves) or GP separators (Fig. 4a, red curves). In both cases the capacity fading continued without any improvement after the replacement of the separator. To the contrary, when the fresh electrode, which performed only one formation cycle, was combined with a GF separator which was withdrawn from the cell after severe capacity fading, it maintained most of its capacity (Fig. 4b). This means that the GF separator acts as an additive

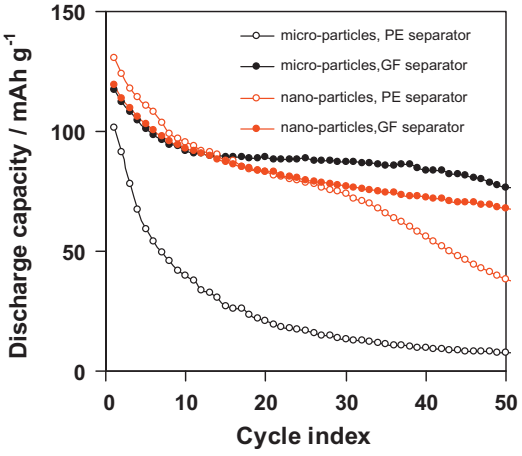

Fig. 2. Curves of discharge capacity vs. cycle number obtained upon galvanostatic cycling (C/5 rates) of $LiCoPO_4$ electrodes prepared from carbon-coated micro- and nano-powders of $LiCoPO_4$, as indicated, in 1 M $LiPF_6$/EC-DMC solution with two types of separators (30 °C).

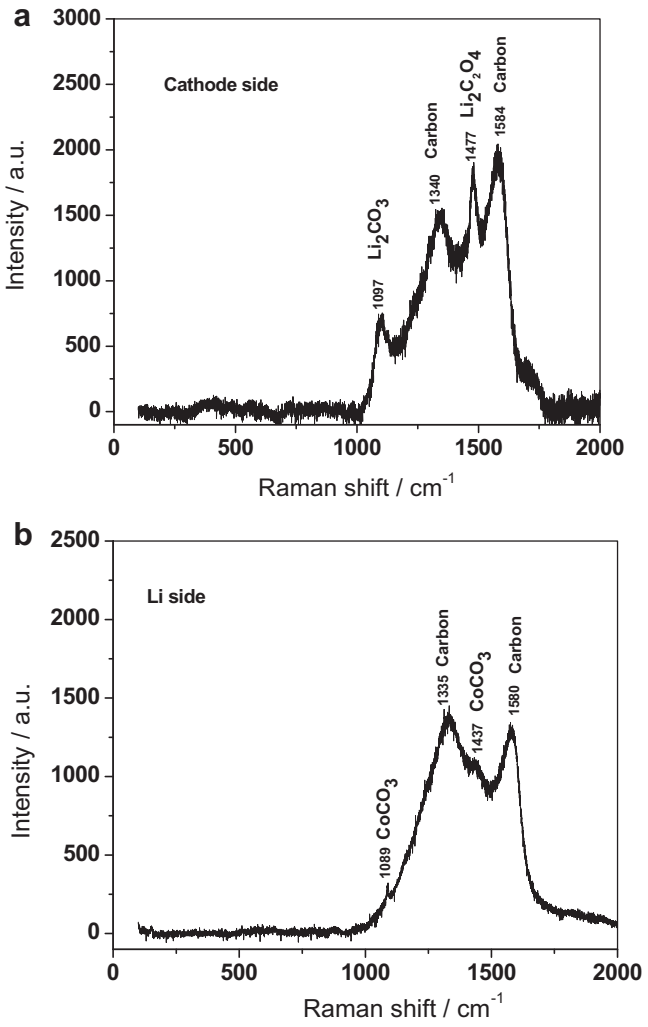

Fig. 3. Micro-Raman spectra of the particles trapped in the PE separator from the cathode side (a) and anode side (b).

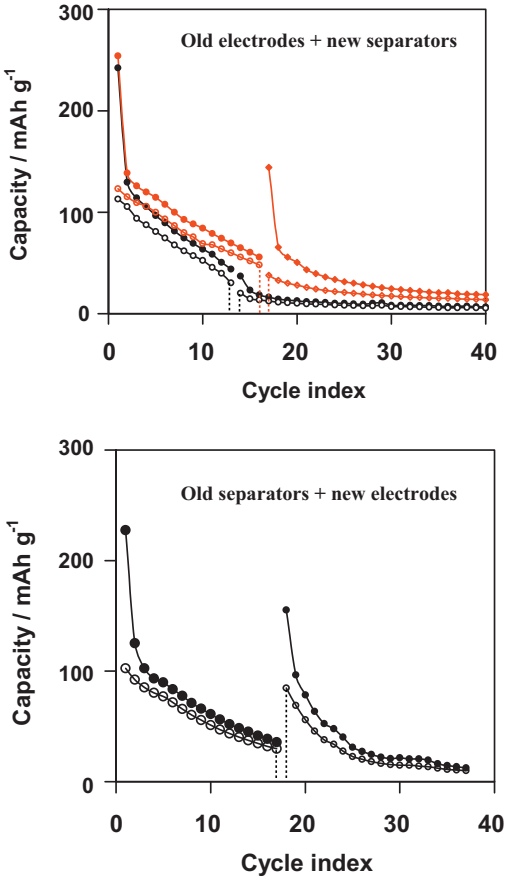

Fig. 4. Curves of charge and discharge capacity vs. cycle number, obtained upon galvanostatic cycling (C/5 h rates) of $LiCoPO_4$ electrodes in the cells with PE separators. (a) After a distinctive decrease in capacity, the PE separators were removed and replaced for a fresh PE (black curves) or GF (red curves) separators. (b) The PE separator was transferred from the cell after a distinct capacity fading to a new $LiCoPO_4$ electrode. (For interpretation of the references to color in this figure legend, the reader is referred to the web version of this article.)

to the electrolyte solution, which prevents the detrimental effect of its components on the cycling performance of $LiCoPO_4$ cathodes. It is well known that SiO_2, the main component of glassy fibers, possesses HF-scavenging properties. The substantial improvement in the capacity retention observed in the presence of GF separators, most probably, relates to the removal of HF which presence in solution is damaging the cathode material.

In fact, the reaction between HF and SiO_2 containing species produces water that can further react with the salt to form more HF, in regenerative process. However, it is logical to assume that scavenging HF by the SiO_2 containing separators in the cells is much faster than its regeneration by the further reaction of trace water thus formed, because HF is formed only by reaction between trace H_2O and PF_5 (formed by thermal decomposition of $LiPF_6$) [17]. The concentration of PF_5 in solutions is supposed to be negligible compared to the amount of SiO_2 containing species in the cells. Thereby, we assume correctly that the use of quartz or glassy paper separators, leads to a pronounced reduction of the trace HF in the cells.

As one can see from Fig. 2, the higher is the surface area of the cathode powder, the slower is the capacity fading of the cells with the PE separators. We can suggest that as the specific surface area of the cathode material is higher, it reacts effectively with all the HF in solution and yet leaves active mass that was not spoiled due to reactions with HF. Hence, in the case of nano-sized cathode powder, a higher portion of the surface layer of the cathode particles remains

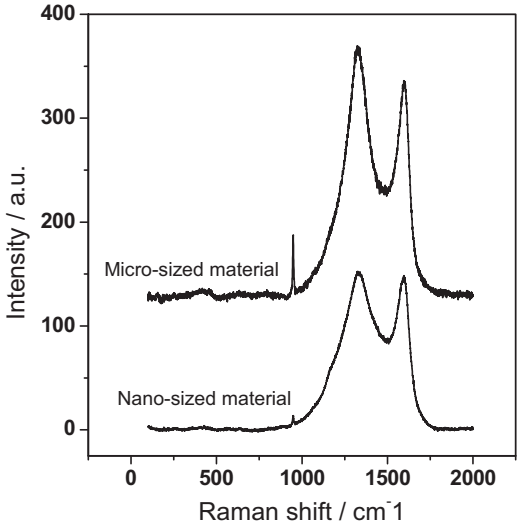

Fig. 5. Raman spectra collected from the pristine electrodes prepared from micro- and nano-$LiCoPO_4$ powder with 633 cm^{-1} He–Ne laser at laser power of 0.37 mW.

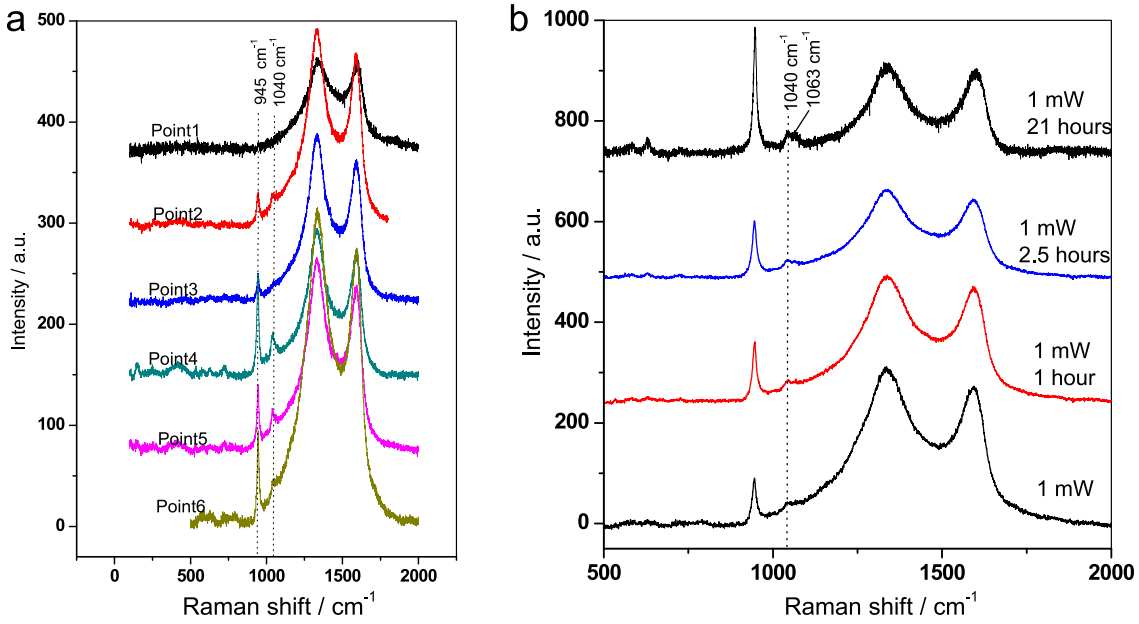

Fig. 6. Raman spectra collected from the electrode prepared from micro-$LiCoPO_4$ powder after prolonged galvanostatic cycling in $LiCoPO_4$/Li cell with PE separator with 633 cm^{-1} He–Ne laser at laser power of 1 mW. (a) Spectra collected from 6 arbitrary points on the surface of the electrode. (b) Spectra collected from the point 6 during prolonged exposure to laser beam.

undamaged in the initial cycling period, because of the scavenging effect of the high surface area. It is important to note that with the olivine cathode materials, we see indeed positive effects of the nanometric particle size for solid state diffusion, fast interfacial charge transport and the effect of HF scavenging discussed herein. This is due to the relatively low basicity and nucleophilicity of the surface oxygen atoms of $LiMPO_4$ compounds (in contrast to the case of lithiated transition metal oxides cathodes, where nano structure of the particles may leads to pronounced surface reactivity of the cathode materials).

As we showed in [18], fast capacity fading, which is observed in the absence of HF scavengers, is the result of the degradation of the olivine structure of the cathodes, accompanied by amorphization and lithium depletion. In this case Raman spectroscopy may be helpful for investigating the structural changes of $LiCoPO_4$ cathode material. Amorphous products of the cathode material which

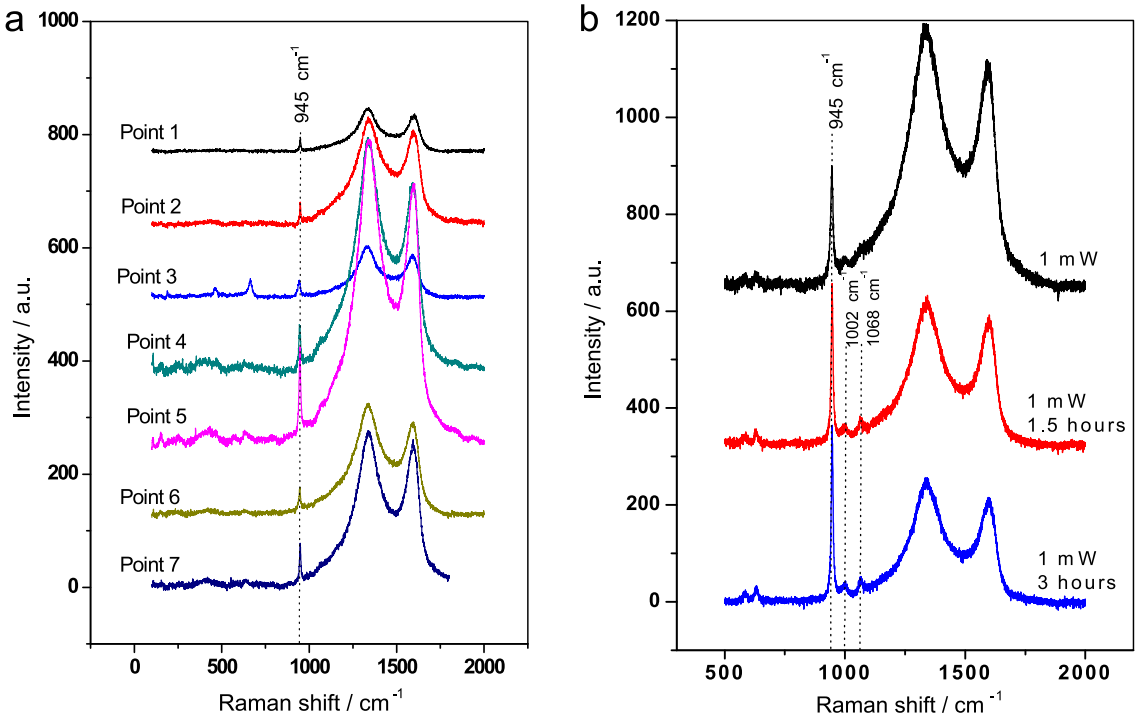

Fig. 7. Raman spectra collected from the electrode prepared from micro-$LiCoPO_4$ powder after prolonged galvanostatic cycling in $LiCoPO_4$/Li cell with GF separator with 633 cm^{-1} He–Ne laser at laser power of 1 mW. (a) Spectra collected from 7 arbitrary points on the surface of the electrode. (b) Spectra collected from the point 8 during prolonged exposure to laser beam.

detection with X-ray techniques is impossible can be probed well by Raman spectroscopy. Fig. 5 presents Raman spectra of pristine electrodes prepared from micro- and nano-particles of $LiCoPO_4$ collected with He–Ne laser at a laser power of 0.37 mW. The carbon layer makes it difficult to see the details of the spectrum of the olivine structure due to the attenuation of the signal by the carbon layer and the overlapping of the spectral bands. Only a weak signal at 945 cm^{-1} related to PO_4^{3-} anion symmetric stretching (the strongest peak of the olivine spectrum) is observed. Using our conclusion that the removal of carbon coating layer under moderate power of the laser beam can provide information about the $LiCoPO_4$ structure [12], we undertook Raman investigation of the cycled composite electrodes.

The electrodes prepared from micro- and nano-particles of $LiCoPO_4$ were cycled in the identical conditions (75 cycles) with two types of separators, PE and GF. For the cells with GF separators one additional layer of PE separator was inserted from the cathode side to prevent the cathode surface from the contamination by the components of GF separator and penetration of dendrites from the lithium counter electrode to the cathode side [18].

Fig. 6a shows Raman spectra collected from 6 arbitrary points on the surface of a $LiCoPO_4$ electrode prepared from micro-powder after prolonged galvanostatic cycling and full capacity fading in $LiCoPO_4$/Li cell with PE separator. One can see that at 1 mW laser power, in the most of the measured points, a weak peak at about 1040 cm^{-1} is observed which is not related to $LiCoPO_4$ olivine structure, along with the olivine band at 945 cm^{-1}. Prolonged exposure to the laser beam of one of the points is shown in Fig. 6b. After the removal of carbon this new band is clearly seen.

Quite different picture is observed for the electrodes prepared from micro-powder of $LiCoPO_4$, but cycled in the presence of GF separator (Fig. 7). In none of the points, band 1040 cm^{-1} was observed, and after the partial removal of carbon layer during prolonged exposure to the laser beam, a distinct olivine spectrum appears. The sharp band at 950 cm^{-1} is attributed to the A_g mode of ν_1 (intra-molecular symmetric vibrations of the PO_4^{3-} anion), while the two weaker bands (1002 and 1070 cm^{-1}) belong to the asymmetric stretching modes of the PO_4^{3-} anion (ν_3) [19].

Similar data were obtained for the cycled electrodes prepared from nano-sized $LiCoPO_4$ powder (Fig. 8). Two typical spectra for the electrodes cycled with two types of separators collected at a laser power of 2.5 mW illustrate the same phenomenon. The olivine structure of $LiCoPO_4$ remains unchanged after cycling with glassy fiber separators (Fig. 8b) and degrades after cycling with PE separators (Fig. 8a). Two bands at 1002 and 1070 cm^{-1} related to the olivine structure disappear and the sharp peak at 1040 cm^{-1} discloses. Another new feature in the spectrum is the band at 725 cm^{-1}. These two new bands fit well to the characteristic features of pyrophosphate compounds with P_2O_7 units, in which two phosphorus atoms are connected to each other via an oxygen bridge [20,21]. The band at 1040 cm^{-1} relates to stretching of the terminal (external) P—O bonds in the pyrophosphate structure, and the band at 725 cm^{-1} corresponds to the bridging P—O stretching [21].

The XRD patterns of the pristine and cycled $LiCoPO_4$ electrodes prepared both from micro- and nano-particles are shown in Fig. 9. It is seen that the electrodes cycled with the GF separators retained their olivine structure, whereas the electrodes after cycling with the PE separators undergo amorphization.

The formation of $Co_2P_2O_7$ was described in [22] as a result of thermal decomposition of lithium-poor phases, Li_zCoPO_4 and $CoPO_4$. It was shown with the use of the in situ synchrotron diffraction technique that the formation of the crystalline $Co_2P_2O_7$ proceeds not simultaneously with the decomposition of these two crystalline phases but rather with a slight delay. The authors of Ref. [21] suggested two possible reaction paths to explain this observation. The first one was amorphization of a lithium-deficient phases

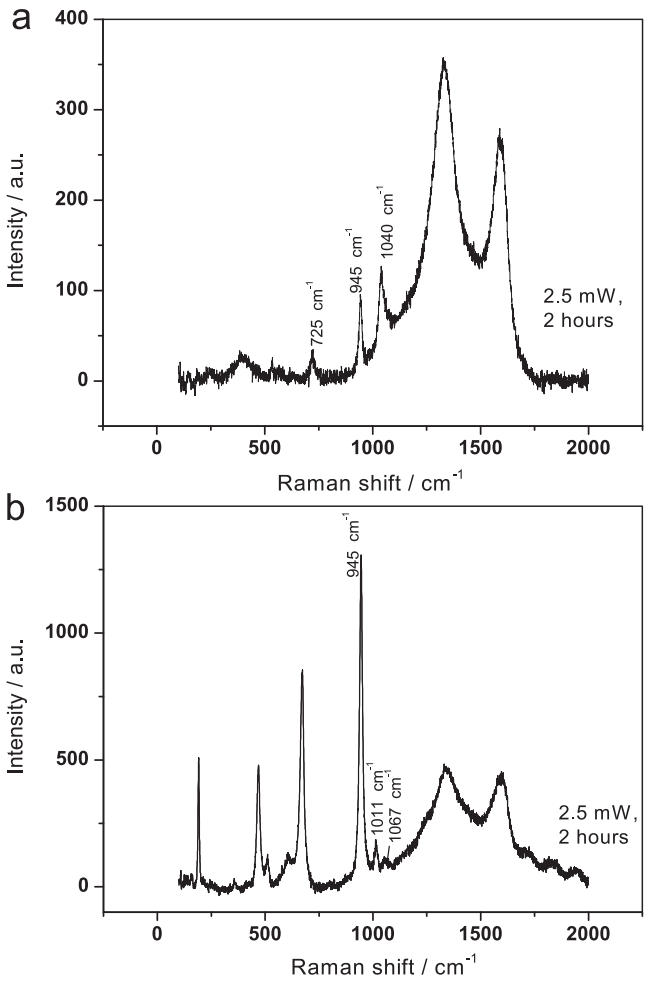

Fig. 8. Typical Raman spectra collected from two electrodes prepared from nano-$LiCoPO_4$ powder after prolonged galvanostatic cycling in $LiCoPO_4$/Li cells with 633 cm^{-1} He–Ne laser at laser power of 2.5 mW. (a) Spectrum collected from the electrode after cycling in $LiCoPO_4$/Li cells with PE separator. (b) Spectrum collected from the electrode after cycling in $LiCoPO_4$/Li cells with GF separator.

with subsequent formation of crystalline $Co_2P_2O_7$, and the second one was decomposition of lithium-deficient phases with formation of amorphous $Co_2P_2O_7$ followed its further crystallization. In either cases, the formation of crystalline pyrophosphate proceeds via the formation of amorphous delithiated phase of the active mass.

In our case we can consider two possible ways of the formation of pyrophosphate. The first one is a degradation of the olivine structure during prolonged cycling of $LiCoPO_4$ electrodes with the formation of pyrophosphate. The second possible reason for the appearance of the pyrophosphate bands in the Raman spectra is the degradation of the amorphous delithiated material under the laser beam of the Raman spectrometer. In any event, the appearance of pyrophosphate features at almost all of the arbitrary points on the surface of the electrodes cycled with PE separators testifies that a total structural degradation of the electrode material occurs during prolonged cycling of these electrodes. At the same time, after the cycling with HF-scavenging GF separators the olivine structure of $LiCoPO_4$ electrodes survived both in the bulk and at the surface of the active mass. Thus, the most probable reason for the capacity fading of $LiCoPO_4$ cathodes in $LiPF_6$ containing solutions is the reactivity of HF towards the olivine compound. We proposed the following mechanism of their interactions which leads to destruction of the structure of $LiCoPO_4$ [23]:

$$PO_4^{3-} + HF + H^+ \leftrightarrow PO_3F^{2-} + H_2O$$

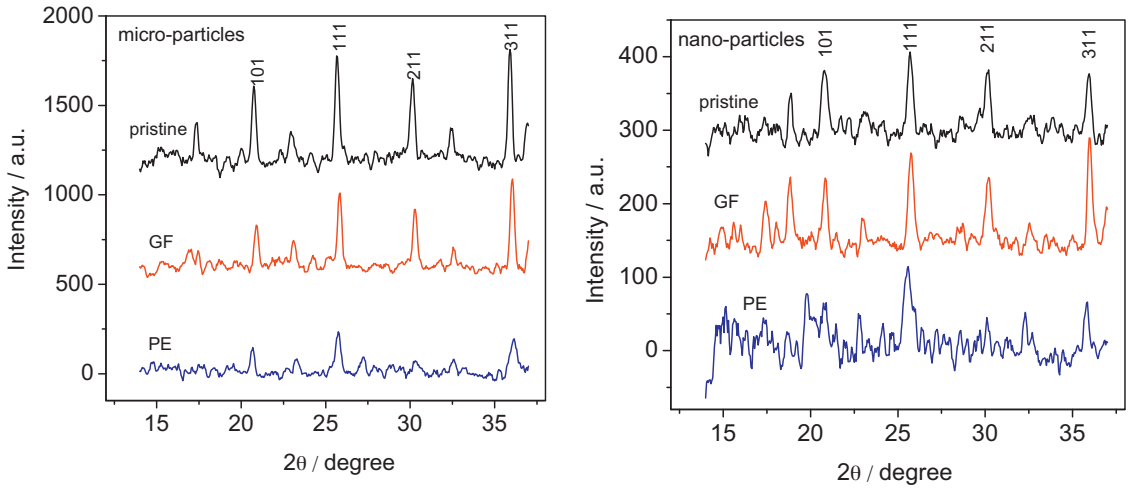

Fig. 9. XRD patterns of $LiCoPO_4$ pristine electrode (black) and electrodes after cycling in the cells with GF (red) PE and separators (blue). (a) Electrodes prepared from micro-particles of $LiCoPO_4$. (b) Electrodes prepared from nano-particles of $LiCoPO_4$. (For interpretation of the references to color in this figure legend, the reader is referred to the web version of this article.)

$$PO_3F^{2-} + HF + H^+ \leftrightarrow PO_2F_2^- + H_2O$$

$$PO_2F_2^- + HF + H^+ \leftrightarrow POF_3 + H_2O$$

We suggest that the prominent difference in the cycling performance of $LiCoPO_4$ and other $LiMPO_4$ compounds (M = Fe or Mn) is due to the high instability of the delithiated form of this olivine, $CoPO_4$. This compound is extremely unstable both thermally and chemically [22,24] and undergoes amorphization in contact with air or moisture. As was shown in [24], the reason for such instability may be the fact that, unlike the other olivines, in $CoPO_4$ Co^{3+} exists in high-spin configuration [24]. Obviously, chemical instability of this compound towards HF leads to the degradation of $LiCoPO_4$ electrodes during their polarization. The exact mechanism of the detrimental action of HF on the $LiCoPO_4$ structure is under investigation.

4. Conclusions

Micro-probe Raman spectroscopy in combination with XRD analysis established that the main reason for the fast capacity fading of $LiCoPO_4$ electrodes cycled in $LiPF_6$ EC/DMC electrolyte solution is the degradation of the olivine structure. The use of HF scavenging GF separator prevents this destructive process to a great extent. We assign fast capacity fading of $LiCoPO_4$ cathodes in $LiPF_6$ containing electrolyte solutions to the reactivity of HF towards this compound, especially the unstable delithiated form of $LiCoPO_4$. In this case, the use of HF scavenging additives can be very helpful for the improvement of the performance of $LiCoPO_4$ electrodes. Development of new electrolyte solutions for this cathode material is in progress.

References

[1] A.K. Padhi, K.S. Nanjundaswamy, J.B. Goodenough, J. Electrochem. Soc. 144 (1997) 1188–1194.
[2] K. Amine, H. Yasuda, M. Yamachi, Electrochem. Solid State Lett. 3 (2000) 178–179.
[3] J. Wolfenstine, U. Lee, B. Poese, J.L. Allen, J. Power Sources 144 (2005) 226–230.
[4] N.N. Bramnik, K.G. Bramnik, T. Buhrmester, C. Bachtz, E. Ehrenberg, H. Fuess, J. Solid State Electrochem. 8 (2004) 558–564.
[5] B. Jin, H.B. Gu, K.W. Kim, J. Solid State Electrochem. 12 (2008) 105–111.
[6] H.H. Li, J. Jin, J.P. Wei, Z. Zhou, J. Yan, Electrochem. Commun. 11 (2009) 95–98.
[7] F. Wang, J. Yang, Y. NuLi, J. Wang, J. Power Sources 195 (2010) 6884–6887.
[8] L. Tan, Z. Luo, H. Liu, Y. Yu, J. Alloys Compd. 502 (2010) 407–410.
[9] J. Wolfenstine, J. Power Sources 158 (2006) 1431–1435.
[10] J. Wolfenstine, J. Read, J.L. Allen, J. Power Sources 163 (2007) 1070–1073.
[11] N.N. Bramnik, K. Nikolowski, C. Baehtz, K.G. Bramnik, H. Ehrenberg, Chem. Mater. 19 (2007) 908–915.
[12] E. Markevich, R. Sharabi, O. Haik, V. Borgel, G. Salitra, D. Aurbach, G. Semrau, M.A. Schmidt, N. Scall, C. Stinner, J. Power Sources 196 (2011) 6433–6439.
[13] G. Nuspl, L. Wimmer, M. Eisgruber, US Patent 2007/0054187 A1 (2007).
[14] F. Tuinstra, J.L. Koenig, J. Chem. Phys. 53 (1970) 1126–1130.
[15] E. Markevich, E. Pollak, G. Salitra, D. Aurbach, J. Power Sources 174 (2007) 1263–1269.
[16] Yu. A. Popkov, A.P. Mokhir, N.A. Sergienko, Fizika Tverdogo Tela 18 (1976) 2053–2058.
[17] T. Kawamura, S. Okada, J. Yamaki, J. Power Sources 156 (2006) 547–554.
[18] R. Sharabi, E. Markevich, V. Borgel, G. Salitra, D. Aurbach, G. Semrau, M.A. Schmidt, N. Schall, C. Stinner, Electrochem. Commun. 13 (2011) 800–802.
[19] W. Paraguassu, P.T.C. Freire, V. Lemos, S.M. Lala, L.A. Montoro, J.M. Rosolen, J. Raman Spectrosc. 36 (2005) 213–220.
[20] J.D. Termine, D.R. Lundy, Calcif. Tissue Res. 15 (1974) 55–70.
[21] L. Popovic, D. de Waal, J.C.A. Boeyens, J. Raman Spectrosc. 36 (2005) 2–11.
[22] N.N. Bramnik, K. Nikolowski, D. Trots, H. Ehrenberg, Electrochem. Solid State Lett. 11 (2008) A89–A93.
[23] E. Markevich, R. Sharabi, H. Gottlieb, V. Borgel, K. Fridman, G. Salitra, D. Aurbach, G. Semrau, M.A. Schmidt, N. Schall, C. Bruenig, Electrochem. Comm. (2011), doi:10.1016/j.elecom.2011.11.014.
[24] H. Ehrenberg, N.N. Bramnik, A. Senyshyn, H. Fuess, Solid State Sci. 11 (2009) 18–23.